Formation of Neutral and Cationic Methyl Derivatives of Titanium Containing Cyclopentadienyl and Aryloxide Ancillary Ligation

Andrew E. Fenwick, Khamphee Phomphrai, Matthew G. Thorn, Jonathan S. Vilardo, Christine A. Trefun, Brigitte Hanna, Phillip E. Fanwick, and Ian P. Rothwell*

Department of Chemistry, Purdue University, 560 Oval Drive, West Lafayette, Indiana 47907-2084

Received August 28, 2003

The series of dimethyltitanium compounds [CpTi(OAr)Me_2], ligated by one cyclopentadienyl (Cp) and one 2,6-disubstituted aryloxide (OAr), have been prepared by the reaction of [CpTi(OAr)Cl_2] with 2 equiv of LiMe or by the addition of parent phenol (HOAr) to a cold ether solution of [$CpTiMe_3$]. The compounds are stable, except for those containing less bulky *o*-methyl substituents; the compounds [CpTi($OC_6H_2Me_2$-2,6-X-4)Me_2] (X = H (**19**), Br (**20**)) undergo ligand exchange to produce [CpTi($OC_6H_2Me_2$-2,6-X-4)$_2$Me] (X = H (**22**), Br (**23**)) and [$CpTiMe_3$]. X-ray crystal structures have been obtained for the dimethyl compounds [CpTi(OC_6H_2Np-2-Bu$^t_2$-4,6)Me_2] (**13**), [CpTi(OC_6H_2{$C_{10}H_9$}-2-Bu$^t_2$-4,6)Me_2] (**14**), [Cp*Ti(OC_6HPh_2-2,6-Bu$^t_2$-3,5)Me_2] (**15**), [CpTi(OC_6Ph_4-2,3,5,6-Br-4)Me_2] (**18**), [CpTi($OC_6H_2Me_2$-2,6-Br-4)Me_2] (**20**), [CpTi(OC_6H_3Pr$^i_2$-2,6)Me_2] (**21**), and the monomethyl species **23**. Reaction of the dimethyl compounds with [$B(C_6F_5)_3$] generates the corresponding cationic methyl species [CpTi(OAr)Me][$MeB(C_6F_5)_3$]. The compound [CpTi(OC_6HPh_4-2,3,5,6)Me][$MeB(C_6F_5)_3$] (**27**) was studied via solution VT-NMR spectroscopy, and the free energy of activation for methyl exchange was estimated to be 14.4(5) kcal mol^{-1} at 10 °C. These thermally unstable cationic derivatives readily eliminate methane at room temperature, affording compounds of the type [CpTi(OAr)(C_6F_5){$CH_2B(C_6F_5)_2$}]. A kinetic study of the conversion of **27** to [CpTi(OC_6HPh_4-2,3,5,6)(C_6F_5){$CH_2B(C_6F_5)_2$}] (**31**) was undertaken. Toluene-d_8 solutions of **27** were found to cleanly convert to **31** and methane, as monitored by ^{1}H NMR spectroscopy. A first-order rate constant of [7.6(2)] × 10^{-4} s^{-1} was measured at 25.0(5) °C. The solid-state structure of [CpTi(OC_6HPh_2-2,6-Me_2-3,5)(C_6F_5)(CH_2B{C_6F_5}$_2$)] (**28**) confirms this formulation and reveals a trigonal-planar boron atom exhibiting no interaction with the adjacent Ti−C_6F_5 unit.

Introduction

There has been a great degree of success reported relating to the use of the group 4 metallocenes as olefin polymerization catalyst precursors.[1] Cationic alkyl complexes of the type [Cp_2MR]$^+$ (M = Ti, Zr, Hf), formed via activation of dihalides or dialkyl complexes [Cp_2MR_2] with MAO or other cocatalysts such as [$B(C_6F_5)_3$] and [Ph_3C][$B(C_6F_5)_4$], are now known to be the catalytically active species in metallocene-based olefin polymerization systems. This highly electrophilic 14-electron species possesses a very complex reaction chemistry, in which the formation of temporarily dormant, stabilized adducts plays a key role. In contrast to heterogeneous Ziegler−Natta catalysts, the homogeneous metallocene-based polymerization catalysts allow reactivity to take place at predominantly a single-metal site that has a well-defined coordination environment. This allows for a relationship to exist between the metallocene structure and the properties of the resulting polyolefin. Through changes in the coordination environment surrounding the metal center, efficient control over properties such as molecular weight (M_w), molecular weight distributions (M_w/M_n), stereochemical microstructure, crystallization behavior, and comonomer incorporation has been achieved. These group 4 metallocene catalysts have greatly enhanced the range and versatility of a variety of types of polyolefin materials, making their role in industrial processes an ever-increasing one.

With the great success of group 4 metallocene olefin polymerization catalysts has come an intense interest in the development of related homogeneous catalysts supported by non-Cp ancillary ligation.[2−4] Many different types of ligand systems have been employed, including macrocycles and porphyrins, meeting with varying degrees of success in terms of their control over polymer properties. Some ligand systems have attracted more attention than others, due to their favorable comparisons with known metallocene systems in terms of this control as well as activity. These include the "con-

* To whom correspondence should be addressed. E-mail: rothwell@purdue.edu.

(1) (a) Bochmann, M. *J. Chem. Soc., Dalton Trans.* **1996**, 255. (b) Brintzinger, H.-H.; Fischer, D.; Mülhaupt, R.; Rieger, B.; Waymouth, R. M. *Angew. Chem., Int. Ed. Engl.* **1995**, *34*, 1143. (c) Möhring, P. C.; Coville, N. J. *J. Organomet. Chem.* **1994**, *479*, 1. (d) Kaminsky, W.; Kulper, K.; Brintzinger, H. H. *Angew. Chem., Int. Ed. Engl.* **1985**, *24*, 507.

10.1021/om0341404 CCC: $27.50
Publication on Web 04/01/2004

strained geometry" [5] and chelating diamide[2a−d,i,j] based catalyst systems.

A variety of ligand systems based upon alkoxide or aryloxide ligands have also been examined. This has included the use of chelating phenoxide[3,4,6] and alkoxide[7] ligands. For example, Schaverien et al. have shown that excellent stereocontrol of the resulting polymer can be achieved using a chelating binaphthoxide catalyst.[3a] A number of "constrained geometry" type catalysts containing oxygen atom linkages to the metal center have also been designed and studied.[5b,8] Finally, a number of ligand systems consisting of monodentate aryloxide− or alkoxide−metal linkages have been studied. This includes results from our group on the isolation and polymerization chemistry of $[(ArO)_2MR]^+$ species.[9] In this paper we report upon the formation and structure of both neutral and cationic methyl compounds of titanium containing both cyclopentadienyl and aryloxide ligation.[10−12] Studies by Nomura et al. have shown that

Scheme 1

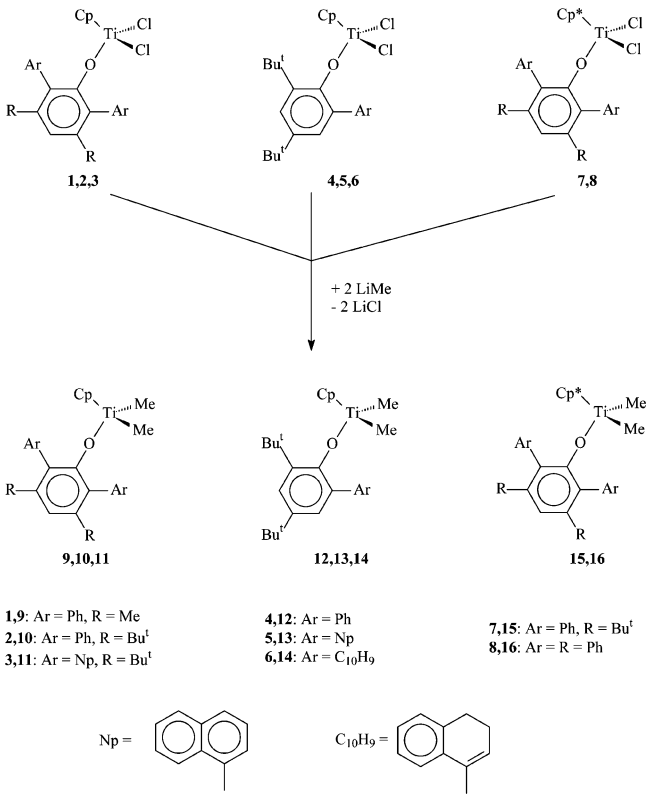

polymerization of ethylene and α-olefins can be achieved with mixed $[Cp(ArO)TiCl_2]$ precursors treated with a variety of activators.[13] In this study emphasis is placed upon the fluxionality of the compounds as well as their thermal stability. Some aspects of this work have been communicated previously.[14]

Results and Discussion

Synthesis and Characterization of Dimethyl Compounds. Treatment of the titanium dichlorides $[Cp(ArO)TiCl_2]$ (**1**−**6**) with 2 equiv of [LiMe] in benzene leads to the corresponding dimethyl compounds **9**−**14** as yellow solids (Scheme 1). Similar treatment of $[Cp^*(ArO)TiCl_2]$ (**7**, **8**) with 2 equiv of [LiMe] afforded the dimethyl compounds **15** and **16**. The 2,3,5,6-tetraphenylphenoxide and 2,6-dimethylphenoxide derivatives **17** and **19** and their corresponding 4-bromo analogues **18** and **20**, as well as the 2,6-diisopropylphenoxide species **21**,[15] were prepared via an alter-

(2) (a) Scollard, J. D.; McConville, D. H. *J. Am. Chem. Soc.* **1996**, *118*, 10008. (b) Tsuie, B.; Swenson, D. C.; Jordan, R. F.; Petersen, J. L. *Organometallics* **1997**, *16*, 1392. (c) Scollard, J. D.; McConville, D. H.; Rettig, S. J. *Organometallics* **1997**, *16*, 1810. (d) Baumann, R.; Davis, W. M.; Schrock, R. R. *J. Am. Chem. Soc.* **1997**, *119*, 3830. (e) Gömez, R.; Green, M. L. H.; Haggitt, J. L. *J. Chem. Soc., Chem. Commun.* **1994**, 2607. (f) Friedrich, S.; Gade, L. H.; Edwards, A. J.; McPartlin, M. *J. Chem. Soc., Dalton Trans.* **1993**, 2861. (g) Brand, H.; Capriotti, J. A.; Arnold, J. *Organometallics* **1994**, *13*, 4469. (h) Aoyagi, K.; Gantzel, P. K.; Kalai, K.; Tilley, T. D. *Organometallics* **1996**, *15*, 923. (i) Cloke, F. G. N.; Geldbach, T. J.; Hitchcock, P. B.; Love, J. B. *J. Organomet. Chem.* **1996**, *506*, 343. (j) Jeon, Y.-M.; Park, S. J.; Heo, J.; Kim, K. *Organometallics* **1998**, *17*, 3161. (k) Horton, A. D.; de With, J.; van der Linden, A. J.; van de Weg, H. *Organometallics* **1996**, *15*, 2672. (l) Shah, S. A. A.; Dorn, H.; Voigt, A.; Roesky, H. W.; Parisini, E.; Schmidt, H.-G.; Noltemeyer, M. *Organometallics* **1996**, *15*, 3176. (m) Herskovics-Korine, D.; Eisen, M. S. *J. Organomet. Chem.* **1995**, *503*, 307.

(3) For the polymerization of olefins by bidentate aryloxides see: (a) van der Linden, A.; Schaverien, C. J.; Meijboom, N.; Grant, C.; Orpen, A. G. *J. Am. Chem. Soc.* **1995**, *117*, 3008. (b) Fokken, S.; Spaniol, T. P.; Kang, H.-C.; Massa, W.; Okuda, J. *Organometallics* **1996**, *15*, 5069. (c) For cationic zirconium alkyls supported by chelating phenoxides see: Cozzi, P. G.; Gallo, E.; Floriani, C.; Chiesi-Villa, A.; Rizzoli, C. *Organometallics* **1995**, *14*, 4994. (d) Bott, R. K. J.; Hughes, D. L.; Schormann, M.; Bochmann, M.; Lancaster, S. J. *J. Organomet. Chem.* **2003**, *665*, 135. (e) Huang, J.; Lian, B.; Qian, Y.; Zhou, W.; Chen, W.; Zheng, G. *Macromolecules* **2002**, *35*, 4871.

(4) Groysman, S.; Goldberg, I.; Kol, M. *Organometallics* **2003**, *22*, 3015 and references therein.

(5) (a) Devore, D. D.; Timmers, F. J.; Hasha, D. L.; Rosen, R. K.; Marks, T. J.; Deck, P. A.; Stern, C. L. *Organometallics* **1995**, *14*, 3132. (b) Chen, Y.-X.; Marks, T. J. *Organometallics* **1997**, *16*, 3649. (c) Duda, L.; Erker, G.; Frohlich, R.; Zippel, F. *Eur. J. Inorg. Chem.* **1998**, 1153. (d) Blais, M. S.; Chien, J. C. W.; Rausch, M. D. *Organometallics* **1998**, *17*, 3775.

(6) (a) Thorn, M. G.; Fanwick, P. E.; Chesnut, R. W.; Rothwell, I. P. *Chem. Commun.* **1999**, 2543. (b) Turner, L. E.; Thorn, M. G.; Fanwick, P. E.; Rothwell, I. P., *Chem. Commun.* **2003**, 1034. (c) Thorn, M. G.; Parker, J. R.; Fanwick, P. E.; Rothwell, I. P. *Organometallics* **2003**, *22*, 4658. (d) Turner, L. E.; Swartz, R. D.; Thorn, M. G.; Chesnut, R. W.; Fanwick, P. E.; Rothwell, I. P. *J. Chem. Soc., Dalton Trans.*, **2003**, 4580. (e) Turner, L. E.; Thorn, M. G.; Fanwick, P. E.; Rothwell, I. P. *Organometallics*, **2004**, *23*, 1576.

(7) Mack, H.; Eisen, M. S. *J. Chem. Soc., Dalton Trans.* **1998**, 917.

(8) Gielens, E. E. C. G.; Tiesnitsch, J. Y.; Hessen, B.; Teuben, J. H. *Organometallics* **1998**, *17*, 1652.

(9) (a) Thorn, M. G., Etheridge, Z. C., Fanwick, P. E., Rothwell, I. P. *Organometallics* **1998**, *17*, 3636. (b) Thorn, M. G.; Etheridge, Z. C.; Fanwick, P. E.; Rothwell, I. P. *J. Organomet. Chem.* **1999**, *591*, 148.

(10) (a) Thorn, M. G.; Vilardo, J. S.; Lee, J. T.; Hanna, B.; Fanwick, P. E.; Rothwell, I. P. *Organometallics* **2000**, *19*, 5636. (b) Vilardo, J. S.; Thorn, M. G.; Fanwick, P. E.; Rothwell, I. P. *Chem. Commun.* **1998**, 2425. (c) Thorn, M. G.; Vilardo, J. S.; Lee, J.; Hanna, B.; Fanwick, P. E.; Rothwell, I. P. *Organometallics* **2000**, *19*, 5636. (d) Thorn, M. G.; Lee, J.; Fanwick, P. E.; Rothwell, I. P. *Dalton* **2002**, 3398. (e) Lee, J.; Fanwick, P. E.; Rothwell, I. P. *Organometallics* **2003**, *22*, 1546.

(11) Sturla, S. J.; Buchwald, S. L. *Organometallics* **2002**, *21*, 739−748.

(12) Firth, A. F.; Stewart, J. C.; Hoskin, A. J.; Stephan, D. W. *J. Organomet. Chem.* **1999**, *591*, 185−193.

(13) (a) Nomura, K.; Oya, K.; Komatsu, T.; Imanishi, Y. *Macromolecules* **2000**, *33*, 3187. (b) Nomura, K.; Oya, K.; Komatsu, T.; Imanishi, Y. *Macromolecules* **2000**, *33*, 8122. (c) Nomura, K.; Okumura, H.; Komatsu, T.; Naga, N. *Macromolecules* **2002**, *35*, 5388. (d) Nomura, K.; Naga, N.; Miki, M.; Yanagi, K. *Macromolecules* **1998**, *31*, 7588. (e) Nomura, K.; Oya, K.; Imanishi, Y. *J. Mol. Catal. A* **2001**, *174*, 127−140. (f) Nomura, K.; Komatsu, T.; Imanishi, Y. *J. Mol. Catal. A* **2000**, *159*, 127−137. (g) Nomura, K.; Komatsu, T.; Imanishi, Y. *J. Mol. Catal. A* **2000**, *152*, 249−252. (h) Nomura, K.; Naga, N.; Miki, M.; Yanagi, K.; Imai, A. *Organometallics* **1998**, *17*, 2152−2154. (i) Imanishi, Y.; Nomura, K. *J. Polym. Sci. A: Polym. Chem.* **2000**, *38*, 4613−4626. (j) Nomura, K.; Fudo, A. *Catal. Commun.* **2003**, *4*, 269−274. (k) Nomura, K.; Tsubota, M.; Fujiki, M. *Macromolecules* **2003**, *36*, 3797−3799. (l) Nomura, K.; Fudo, A. *Inorg. Chim. Acta* **2003**, *345*, 37−43. (m) Nomura, K.; Okumura, H.; Komatsu, T.; Naga, N.; Imanishi, Y. *J. Mol. Catal. A* **2002**, *190*, 225−234.

(14) Thorn, M. G., Vilardo, J. S., Fanwick, P. E., Rothwell, I. P. *Chem. Commun.* **1998**, 2427.

(15) An alternative procedure for the synthesis of **21** has been reported.[12]

Scheme 2

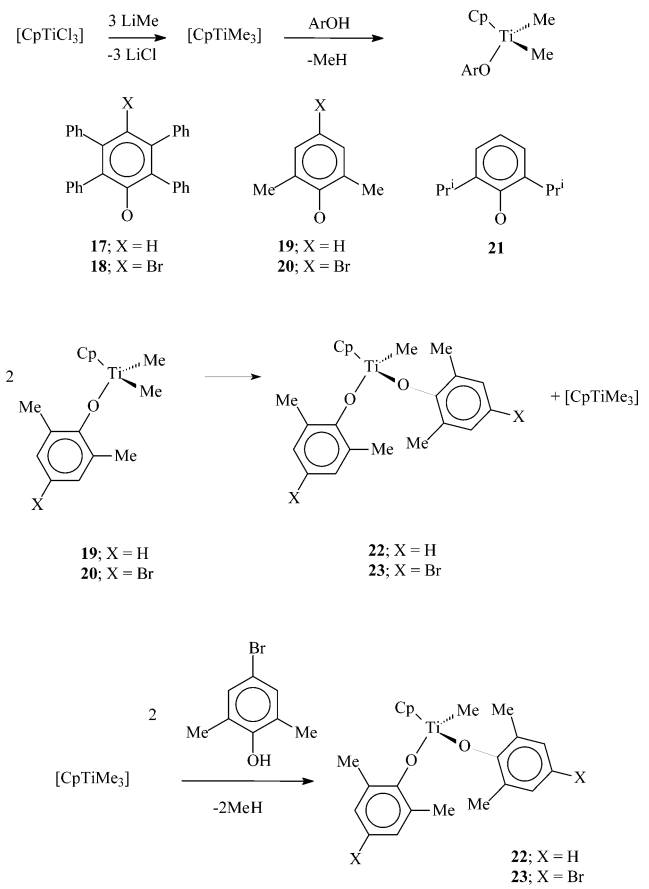

nate procedure (Scheme 2). The in situ synthesis of $[CpTiMe_3]$ (from the addition of 3 equiv of [LiMe] to $[CpTiCl_3]$ in ether at −78 °C) was followed by the addition of the corresponding phenol. The synthesis proceeded in high yield. However, in the case of the 2,6-dimethylphenoxides **19** and **20**, slow decomposition was observed over days to produce (^{1}H NR) mixtures containing the bis(aryloxide) monomethyl species [Cp-Ti($OC_6H_3Me_2$-2,6)$_2$Me] (**22**) and [CpTi($OC_6H_2Me_2$-2,6-Br-4)$_2$Me] (**23**), respectively (Scheme 2). This latter reaction presumably occurs via ligand exchange for the smaller aryloxide ligands. The bis(aryloxide) compounds were also prepared pure via addition of 2 equiv of 2,6-dimethylphenols to $[CpTiMe_3]$ (Scheme 2).

The solid-state structures of dimethyl compounds **13**−**15**, **18**, **20**, and **21** have been determined by single-crystal X-ray diffraction methods. An ORTEP view of each molecule is shown in Figures 1−6, and selected bond distances and angles are collected in Tables 1−6. The solid-state structure of the monomethyl species **23** was also determined (Figure 7, Table 7). Analysis of the Ti−Me distances and Me−Ti−Me angles for titanium

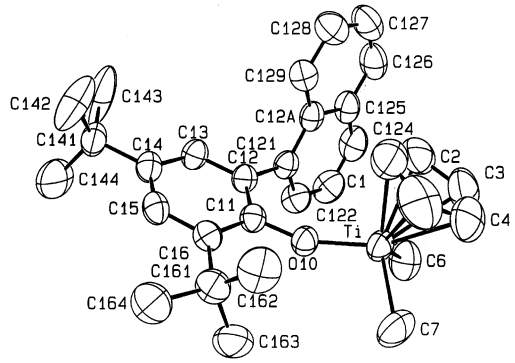

Figure 1. Molecular structure of [CpTi(OC_6H_2Np-2-Bu$^t_2$-4,6)Me_2] (**13**).

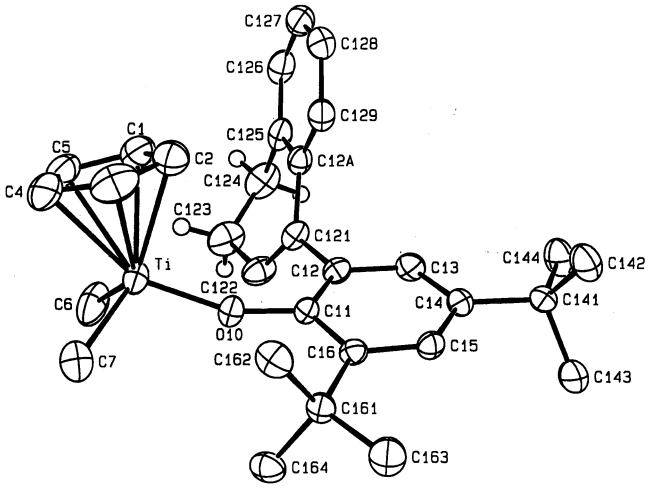

Figure 2. Molecular structure of [CpTi(OC_6H_2{$C_{10}H_9$}-2-Bu$^t_2$-4,6)Me_2] (**14**).

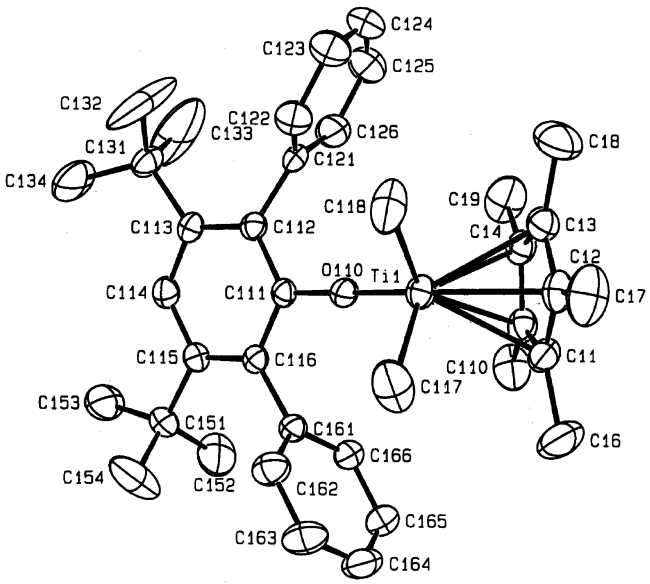

Figure 3. Molecular structure of [Cp*Ti(OC_6HPh_2-2,6-Bu$^t_2$-3,5)Me_2] (**15**).

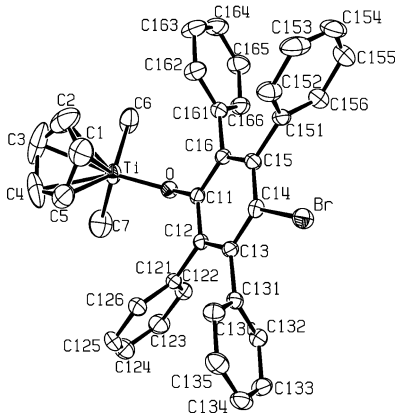

Figure 4. Molecular structure of [CpTi(OC_6Ph_4-2,3,5,6-Br-4)Me_2] (**18**).

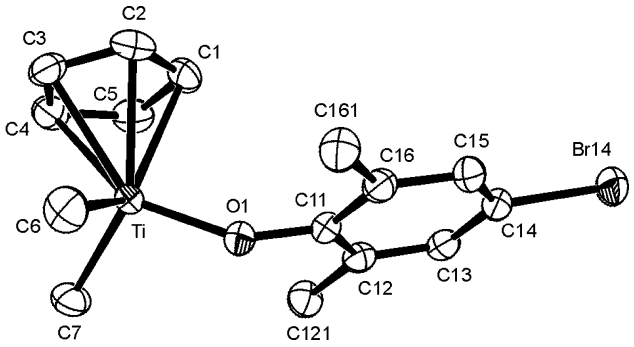

Figure 5. Molecular structure of [CpTi($OC_6H_2Me_2$-2,6-Br-4)Me_2] (**20**).

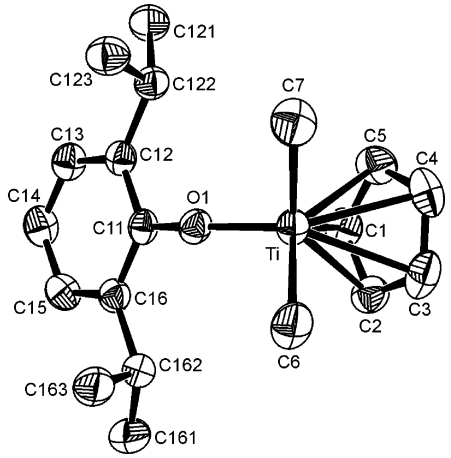

Figure 6. Molecular structure of [CpTi($OC_6H_3Pr^i_2$-2,6)Me_2] (**21**).

Table 1. Selected Bond Distances (Å) and Angles (deg) for [CpTi(OC_6H_2Np-2-Bu^t_2-4,6)Me_2] (13)

Ti-O(10)	1.815(2)	Ti−C(7)	2.091(4)
Ti−C(6)	2.076(4)	Ti−Cp	2.053(5)
Ti−O(10)−C(11)	158.9(2)	C(6)−Ti−C(7)	97.5(2)
O(10)−Ti−C(6)	105.8(1)	C(6)−Ti−Cp	111.0(2)
O(10)−Ti−C(7)	103.8(1)	C(7)−Ti−Cp	111.8(2)
O(10)−Ti−Cp	123.7(2)		

Table 2. Selected Bond Distances (Å) and Angles (deg) for [CpTi{OC_6H_2{$C_{10}H_9$}-2-Bu^t_2-4,6}Me_2] (14)

Ti−O(10)	1.811(2)	Ti−C(6)	2.097(3)
Ti−C(7)	2.103(3)	Ti−Cp	2.044(3)
Ti−O(10)−C(11)	160.1(2)	C(6)−Ti−C(7)	97.7(1)
O(10)−Ti−C(6)	105.6(1)	C(6)−Ti−Cp	111.3(1)
O(10)−Ti−C(7)	103.8(1)	C(7)−Ti−Cp	111.5(1)
O(10)−Ti−Cp	123.7(1)		

Table 3. Selected Bond Distances (Å) and Angles (deg) for [Cp*Ti(OC_6HPh_2-2,6-Bu^t_2-3,5)Me_2] (15)

Ti(1)−O(110)	1.824(2)	Ti(1)−C(118)	2.112(4)
Ti(1)−C(117)	2.088(4)	Ti(1)−Cp*	2.065(4)
Ti(1)−O(110)−C(111)	172.3(2)	C(117)−Ti(1)−C(118)	91.6(2)
O(110)−Ti(1)−C(117)	103.5(1)	C(117)−Ti(1)−Cp*	110.6(2)
O(110)−Ti(1)−C(118)	105.4(1)	C(118)−Ti(1)−Cp*	110.7(2)
O(110)−Ti(1)−Cp*	128.6(1)		

dimethyl compounds [$(X)_2TiMe_2$] has been performed using data from the Cambridge Crystallographic Database (Figure 8). The data on previously reported compounds clearly show that, as a group, titanocene dimethyl compounds based upon either cyclopentadienyl or *ansa*-metallocene ligands have Me−Ti−Me angles <95° and Ti−Me distances in the range 2.12−2.22 Å.

Table 4. Selected Bond Distances (Å) and Angles (deg) for [CpTi(OC_6Ph_4-2,3,5,6-Br-4)Me_2] (18)

Ti−O(1)	1.828(1)	Ti−C(7)	2.089(3)
Ti−C(6)	2.084(2)	Ti−Cp	2.044(5)
Ti−O(1)−C(11)	148.1(1)	C(6)−Ti−C(7)	100.8(1)
O(1)−Ti−C(6)	102.8(1)	C(6)−Ti−Cp	112.7(1)
O(1)−Ti−C(7)	104.6(1)	C(7)−Ti−Cp	112.7(1)
O(1)−Ti−Cp	121.0(1)		

Table 5. Selected Bond Distances (Å) and Angles (deg) for [CpTi($OC_6H_2Me_2$-2,6-Br-4)Me_2] (20)

Ti−O(1)	1.812(1)	Ti−C(7)	2.101(2)
Ti−C(6)	2.088(2)	Ti−Cp	2.046(2)
O(1)−Ti−Cp	120.29(9)	C(6)−Ti−C(7)	100.80(9)
O(1)−Ti−C(6)	103.64(8)	C(6)−Ti−Cp	112.91(9)
O(1)−Ti−C(7)	103.72(7)	C(7)−Ti−Cp	113.21(9)
Ti−O(1)−C(1)	150.0(1)		

Table 6. Selected Bond Distances (Å) and Angles (deg) for [CpTi($OC_6H_3Pr^i_2$-2,6)Me_2] (21)

Ti−O(1)	1.803(2)	Ti−C(7)	2.105(3)
Ti−C(6)	2.103(3)	Ti−Cp	2.045(3)
O(1)−Ti−Cp	120.8(1)	C(6)−Ti−C(7)	101.8(1)
O(1)−Ti−C(6)	104.0(1)	C(6)−Ti−Cp	112.4(1)
O(1)−Ti−C(7)	103.2(1)	C(7)−Ti−Cp	112.6(1)
Ti−O(1)−C(1)	157.5(1)		

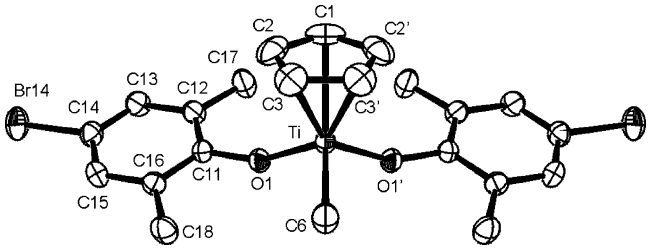

Figure 7. Molecular structure of [CpTi($OC_6H_2Me_2$-2,6-Br-4)$_2$Me] (**23**).

Table 7. Selected Bond Distances (Å) and Angles (deg) for [CpTi($OC_6H_2Me_2$-2,6-Br-4)$_2$Me] (23)

Ti−O(1)	1.816(2)	Ti−Cp	2.043(4)
Ti−C(6)	2.108(4)		
O(1)−Ti−Cp	118.1(1)	O(1)−Ti−O(1)′	107.6(1)
O(1)−Ti−C(6)	100.8(1)	C(6)−Ti−Cp	108.7(1)
Ti−O(1)−C(1)	152.4(2)		

Those dimethyl compounds having either only one cyclopentadienyl ligand (including constrained-geometry ligand systems) or two anionic donor ligands (e.g. amido or aryloxo groups) have a larger Me−Ti−Me angle (>100°) and, on average, slightly shorter Ti−Me distances (2.02−2.14 Å). The distances and angles for **13**, **14**, **18**, **20**, and **21** are very similar and are closer to this latter subgroup of compounds (Figure 8). In contrast, the pentamethylcyclopentadienyl compound [Cp*Ti(OC_6HPh_2-2,6-Bu^t_2-3,5)Me_2] (**15**) has similar Ti−Me distances but a smaller Me−Ti−Me angle. The smaller Me−Ti−Me angle possibly reflects the steric compression by the bulky Cp* and aryloxide ligands but may also be a consequence of the more electron releasing Cp* group. The overall trend in Ti−Me distances can be accounted for in terms of the ligand-dependent electrophilicity of the titanium metal center; that is, more electron-donating cyclopentadienyl ligation leads to longer Ti−Me distances. The Ti−O distances are comparable to those in related Ti(IV) aryloxides, a large number of which have now been structurally character-

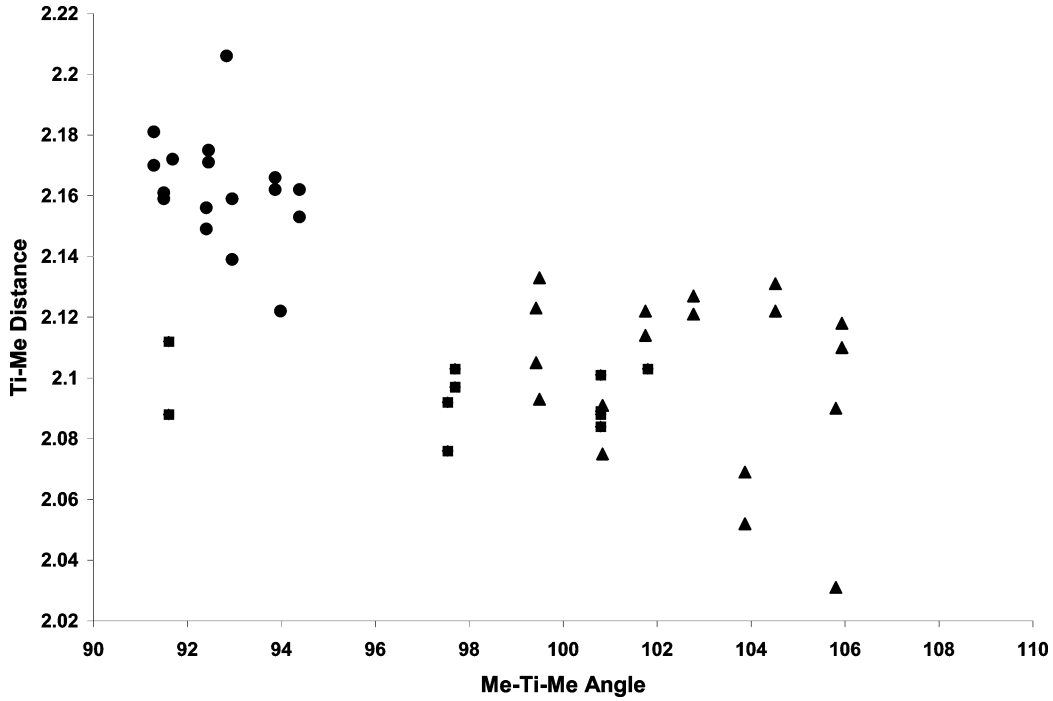

Figure 8. Plot of Ti−Me distances versus Me−Ti−Me angles for dimethyl derivatives of titanium. Bis(cyclopentadienyl) derivatives (●) and other ancillary ligands (▲) are differentiated. Parameters for compounds **13**−**15**, **18**, **20**, and **21** are indicated by ■.

ized. The very large Ti−O−Ar angles are also as expected.[16]

In the solution spectra of **9**, **10**, **12**, and **15**−**21**, only one signal is present for the Ti−Me groups in the ^{1}H and ^{13}C NMR spectra. The chemical shift of the Ti−CH_3 protons is highly dependent upon the nature of the ancillary aryloxide ligand. In particular, an upfield shifting of these protons is observed when *o*-phenyl groups are introduced onto the phenoxide nucleus. The upfield shifting of adjacent ligand protons caused by the diamagnetic shielding of these *o*-phenyl aryloxides has been well documented.[17] Furthermore, the increase in upfield shifting when the *o*-phenyl ring is buttressed by meta substituents is also clearly evident: cf. Ti−CH_3 chemical shifts of δ 0.91, 0.88, 0.33, 0.26, and 0.10 ppm in **19**, **12**, **17**, **9**, and **10**, respectively. The presence of a single Ti−Me resonance for **12** shows that rapid rotation about the Ti−OAr bond is occurring on the NMR time scale.

In contrast, two well-resolved Ti−Me resonances are observed for the *o*-(1-naphthyl) and *o*-(3,4-dihydro-1-naphthyl) derivatives **11**, **13** (Figure 9), and **14**. This is consistent with the presence of the chiral, *dl* form of the 2,6-bis(1-naphthyl)-3,5-di-*tert*-butylphenoxide ligand in **11**. The dramatic upfield shifting of the Ti−CH_3 protons by the large diamagnetic anisotropy of *o*-naphthyl rings is shown by the chemical shifts of δ −0.35 and −0.81 ppm for the methyl signals in the ^{1}H NMR spectrum of **11**. Variable-temperature NMR studies of **13** show that the two methyl signals remain sharp even at 90 °C (toluene-d_8), indicating slow naphthyl rotation on the NMR time scale at this temperature. Previous NMR studies of 2,6-bis(1-naphthyl)phenol have shown the barrier to naphthyl rotation in this molecule can be estimated as 18.0(5) kcal mol^{-1} at 67 °C.[18] Interestingly, both Ti−*Me* groups in the previously reported [CpTi(OC$_6$H$_2${C$_9$H$_7$}-2-Bu$^t_2$-4,6)Me$_2$] appear as one broad singlet in both the ^{1}H and ^{13}C NMR spectra at ambient temperatures but appear as two well-resolved resonances at lower temperatures. This molecule is identical with **13** and **14**, except it contains an *o*-inden-3-yl substituent. From the coalescence temperature the barrier to indenyl rotation can be estimated to be 13.4(5) kcal mol^{-1} at −5 °C. Hence, it is clear that the barrier to naphthyl and dihydronaphthyl rotation is significantly higher than that for indenyl rotation in these directly related compounds.

In all of the dimethyl compounds [CpTi(OAr)Me$_2$], the Ti−*C*H$_3$ carbon atoms resonate in the δ 53−60 ppm region of the ^{13}C NMR spectrum. Highly characteristic single resonances for the Ti−O−*C* ipso carbon (δ 160−164 ppm) and Cp (δ 113−114 ppm) and Cp* ligands (δ 120−122 ppm) were observed in the ^{13}C NMR spectra.

Synthesis and Characterization of Cationic Methyl Compounds. Addition of [B(C$_6$F$_5$)$_3$] to the dimethyl compounds [Cp(ArO)TiMe$_2$] (**9**, **12**, **13**, and **17**) in benzene or toluene solvent led to the rapid formation of the thermally unstable (vide infra) cationic methyl compounds **24**−**27** (Scheme 3). The Ti−*C*H$_3$ methyl carbon resonates in the δ 77−80 ppm region of the ^{13}C NMR spectra for all four compounds, significantly downfield of the parent neutral dimethyl compounds. Variable-temperature NMR spectra of these species are

(16) (a) Bradley, D. C.; Mehrotra, R. C.; Rothwell, I. P.; Singh, A. *Alkoxo and Aryloxo Derivatives of Metals*; Academic Press: London, 2001. (b) Steffey, B. D.; Fanwick, P. E.; Rothwell, I. P. *Polyhedron* **1990**, *9*, 963.

(17) Vilardo, J. S.; Lockwood, M. A.; Hanson, L. G.; Clark, J. R.; Parkin, B. C.; Fanwick, P. E.; Rothwell, I. P. *J. Chem. Soc., Dalton Trans.* **1997**, 3353.

(18) (a) Vilardo, J. S.; Thorn, M. G.; Fanwick, P. E.; Rothwell, I. P. *Chem. Commun.* **1998**, 2425. (b) Thorn, M. G.; Vilardo, J. S.; Fanwick, P. E.; Rothwell, I. P. *Chem. Commun.* **1998**, 2427. (c) Riley, P. N.; Thorn, M. G.; Vilardo, J. S.; Lockwood, M. A.; Fanwick, P. E.; Rothwell, I. P. *Organometallics* **1999**, *18*, 3016.

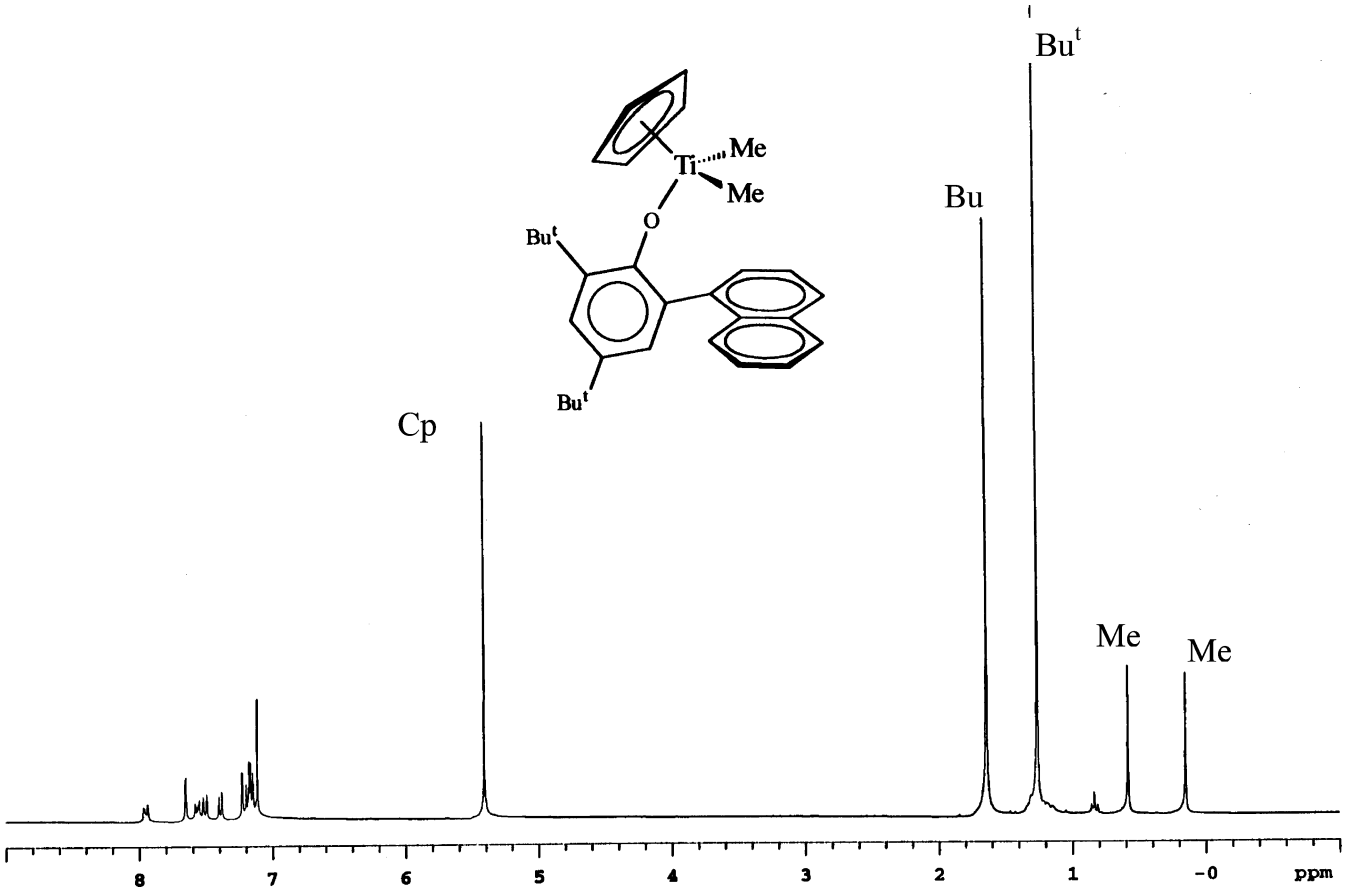

Figure 9. ^{1}H NMR (C_6D_6) spectrum of [CpTi(OC_6H_2Np-2-Bu^t_2-4,6)Me_2] (**13**).

Scheme 3

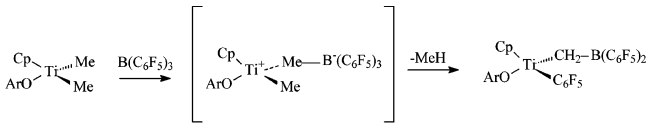

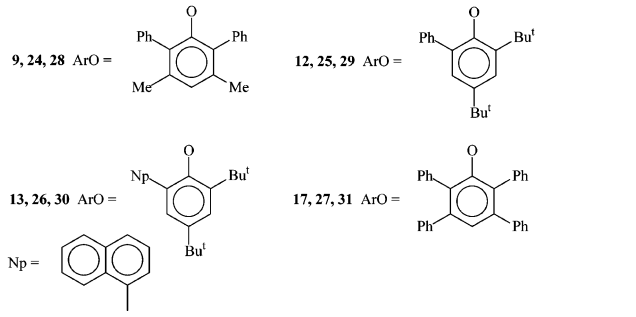

highly informative. Low-temperature ^{1}H and ^{13}C NMR spectroscopy of **24**, **25**, and **27** show a single set of Cp and OAr resonances along with resolved Ti−Me (sharp) and Ti−*Me*−B (broad) signals. Spectra obtained for **25** at ambient temperature show broadening of these methyl signals, but the thermal instability precluded obtaining limiting high-temperature spectra. This broadening was interpreted as being due to exchange of the boron between methyl groups (methyl exchange), which is becoming fast on the NMR time scale. The low-temperature ^{1}H NMR spectra for **27** clearly show well-resolved methyl peaks below 0 °C and a broad singlet at room temperature (Figure 10). On the basis of the spectra obtained for **27**, the free energy of activation for methyl exchange was estimated to be 14.4(5) kcal mol^{-1} at 10 °C.

In the case of **26**, two broad methyl signals as well as a single sharp Cp resonance are observed at room temperature. At −10 °C (toluene-d_8) the Ti−*Me* and Ti−*Me*−B signals sharpen, but there is still only a single Cp resonance. At −30 °C the Cp resonance splits into two signals in a ratio of 80:20, representing the two diastereomeric forms of **26** (Scheme 4). The methyl signals also split into two large equal-intensity signals and one resolvable smaller peak (presumably a further methyl signal was obscured by aryloxide Bu^t resonances). These changes were interpreted as representing two distinct dynamic processes (Scheme 4). The faster process involves exchange between the two diastereomers (80:20 ratio) of **26** (Scheme 4) without methyl exchange. This process involves cation−anion dissociation and rearrangement and is presumably also occurring for **24**, **25**, and **27** but can only be detected using the chiral *o*-(1-naphthyl)phenoxide. An alternative process for exchange of diastereomers would involve naphthyl rotation within **26**. However, the variable-temperature NMR studies on **13** and data presented for another compound below show that this process is too slow to account for the observed process on the NMR time scale. The slower process in **26**, which is also detected for **24**, **25**, and **27**, involves Ti−*Me*/Ti−*Me*−B exchange. In the case of **26**, this process alone cannot lead to exchange of methyl signals in the NMR spectra. However, when coupled with the faster ion-pair dis-

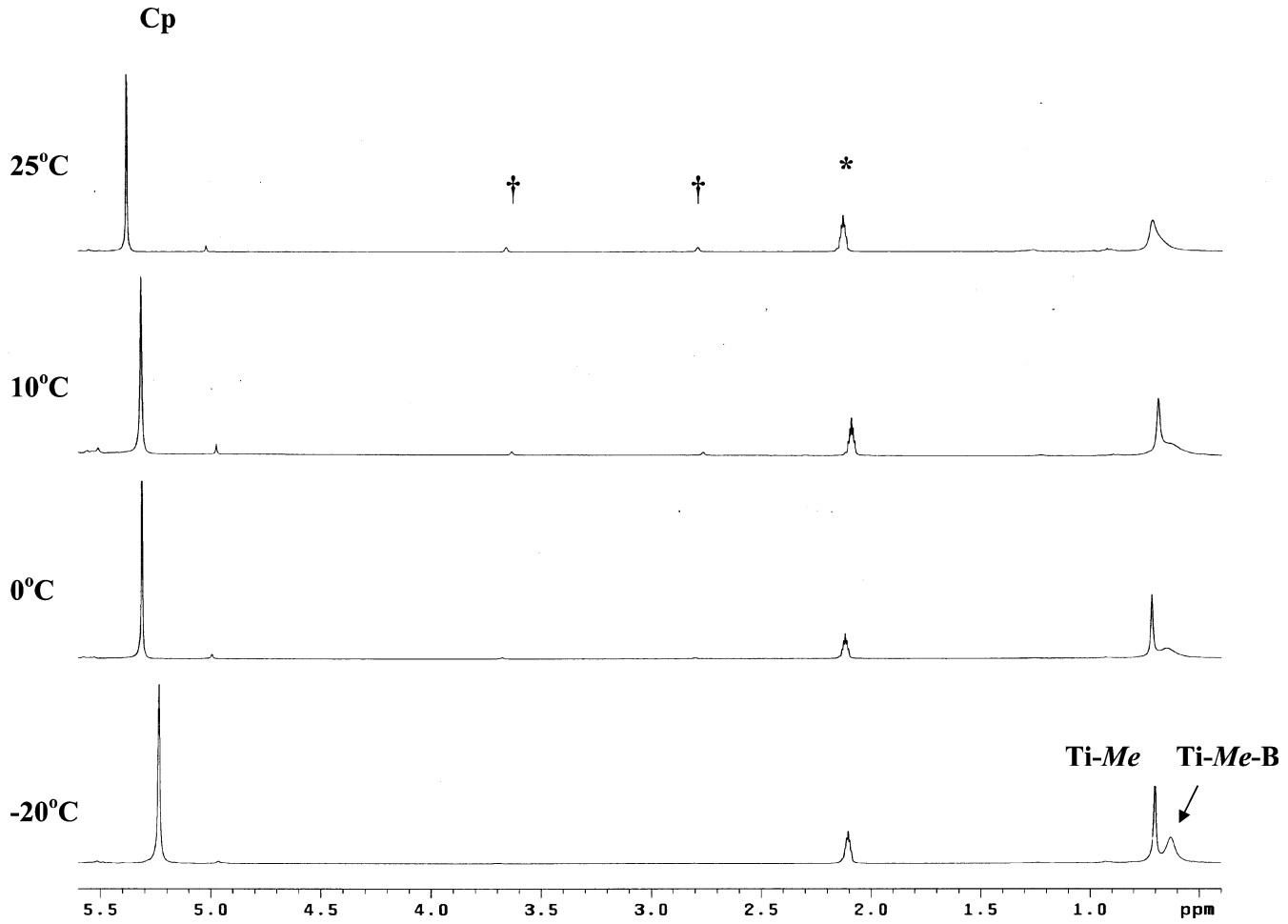

Figure 10. ^{1}H NMR (C_7D_8) spectra of [CpTi(OC_6HPh_4-2,3,5,6)Me][MeB(C_6F_5)$_3$] **27** at 25, 10, 0, and −20 °C. The asterisk (*) indicates the protio impurity of toluene-d_8 solvent, and the daggers (†) indicate the buildup of **31**.

sociation, it leads to diastereotopic methyl exchange. Previous work by Marks et al. has shown similar dynamics are present in [Cp′$_2$Zr(Me){MeB(C_6F_5)$_3$}] species. On the basis of the spectra obtained for **26**, the free energy of activation for ion-pair dissociation was estimated to be 12.4(5) kcal mol^{-1} at −25 °C (Cp coalescence temperature at 300 MHz), while that for the methyl exchange was estimated to be 15.0(5) kcal mol^{-1} at −35 °C.

Decomposition Pathways for the Cationic Methyl Compounds. As discovered by ^{1}H NMR monitoring, solutions of **24**−**27** eliminate methane (determined via NMR) at a rate which is temperature dependent to produce the neutral organometallic species **28**−**31** (Scheme 3). Related reactivity has been observed for the decomposition of other cationic methyl compounds of the group 4 metals where [MeB(C_6F_5)$_3$]$^-$ anions are present. In a particularly important mechanistic study, it was concluded that the reaction occurs via a σ-bond metathesis pathway.[19] Cyclometalation (intramolecular CH bond activation) of aryloxide ligands within cationic group 4 metal alkyls has also been observed.[9] The solid-state structure of **28** confirms the molecular structure and shows that the boron atom is trigonal planar with no interaction present with the adjacent Ti−C_6F_5 unit (Figure 11, Table 8).[2c] The Ti−CH_2B distance of 2.115-

Scheme 4

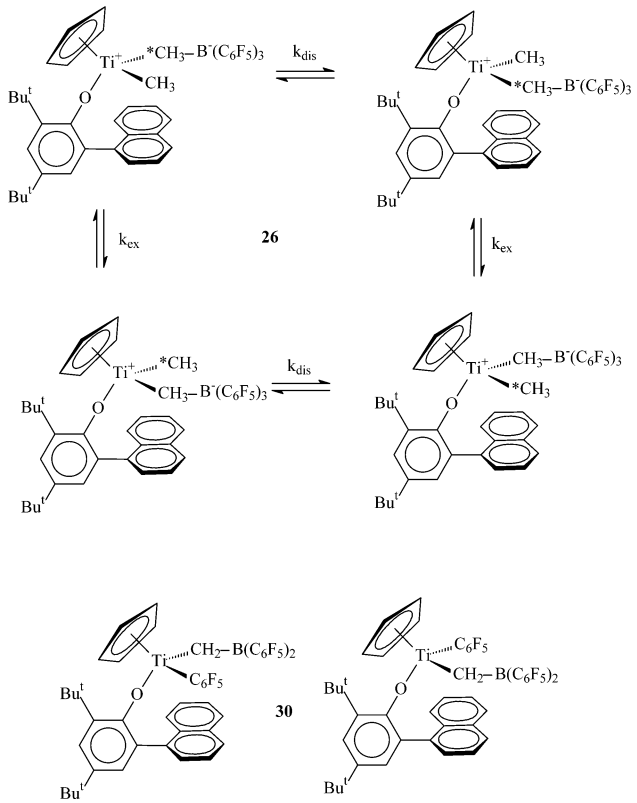

(19) Zhang, S.; Piers, W. E.; Gao, X.; Parvez, M. *J. Am. Chem. Soc.* **2000**, *122*, 5499.

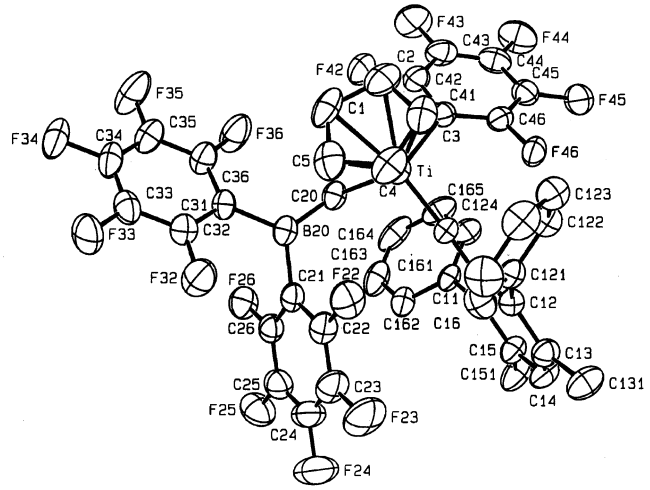

Figure 11. Molecular structure of [CpTi(OC_6HPh_2-2,6-Me_2-3,5)(C_6F_5)($CH_2B\{C_6F_5\}_2$)] (**28**).

Table 8. Selected Bond Distances (Å) and Angles (deg) for [CpTi(OC_6HPh_2-2,6-Me_2-3,5)(C_6F_5)-{$CH_2B(C_6F_5)_2$}] (28)

Ti−O(10)	1.770(2)	B(20)−C(20)	1.495(3)
Ti−C(20)	2.115(2)	B(20)−C(21)	1.595(4)
Ti−C(41)	2.176(2)	B(20)−C(31)	1.594(3)
Ti−Cp	2.044(3)		
Ti−O(10)−C(11)	176.2(1)	C(41)−Ti−Cp	109.7(1)
O(10)−Ti−C(20)	102.44(8)	Ti−C(20)−B(20)	120.0(2)
O(10)−Ti−C(41)	100.25(8)	C(20)−B(20)−C(21)	119.2(2)
O(10)−Ti−Cp	126.9(1)	C(20)−B(20)−C(31)	122.9(2)
C(20)−Ti−C(41)	98.73(8)	C(21)−B(20)−C((31)	117.9(2)
C(20)−Ti−Cp	114.61(9)		

(2) Å in **28** is identical with corresponding distances reported in [CpTi($NHC_6H_3Me_2$)(C_6F_5)($CH_2B\{C_6F_5\}_2$)] (2.165 Å),[20] [($ArNCH_2CH_2CH_2NAr$)Ti(C_6F_5)($CH_2B\{C_6F_5\}_2$)] (2.111 Å),[21] and [CpTi($NHC_6H_3Me_2$)(C_6F_5)($CH_2B\{C_6F_5\}_2$)] (2.183 Å). In the ^{1}H NMR spectra of **28**, **29**, and **31**, a single set of Cp and aryloxide resonances is present along with well-resolved, diastereotopic Ti−CH_2−B protons. In the case of **30**, which contains the chiral *o*-(1-naphthyl) ligand, two sets of sharp NMR signals are present, due to a 70:30 mixture of the two possible diastereomers (Scheme 4). The fact that exchange of these isomers is slow on the NMR time scale at ambient temperature confirms that naphthyl rotation cannot account for the observed fluxionality in **26**.

A kinetic study of the conversion of **27** to **31** was undertaken. Toluene-d_8 solutions of **27**, generated in situ by addition of [$B(C_6F_5)_3$] to **17**, were found to cleanly convert to **31** and methane, as monitored by ^{1}H NMR spectroscopy. Integration of the Cp proton resonances and a plot of ln{[**27**]/([**27**] + [**31**])} vs time showed a first-order decomposition of **27** over approximately 4 half-lives (Figure 12). A first-order rate constant of [7.6(2)] $\times$ 10^{-4} s^{-1} was calculated at 25.0(5) °C; $t_{1/2} \approx 15$ min. The activation of the 2,6-dimethylphenoxide and 2,6-diisopropylphenoxide precursors **19**−**21** with [$B(C_6F_5)_3$] was also found to lead to cationic methyl compounds. However, preliminary studies indicated a different decomposition pathway was present. A detailed study of this alternative deactivation step as well as olefin polymerization studies will be the focus of future reports.

(20) Gomez, R.; Gomez-Sal, P.; del Real, A.; Royo, P. *J. Organomet. Chem.* **1999**, *22*, 588.

(21) Scollard, J. D.; McConville, D. H.; Rettig, S. J. *Organometallics* **1997**, *16*, 1810.

Experimental Section

General Details. All operations were carried out under a dry nitrogen atmosphere using standard Schlenk techniques. The hydrocarbon solvents were distilled from sodium/benzophenone or purified using an Innovative Technologies solvent purification system and were stored over sodium ribbons under nitrogen until use. LiMe was used as received from Aldrich or evaporated to dryness and used without further purification. [$B(C_6F_5)_3$] was purchased from Aldrich, Lancaster, and Strem and used without further purification. The preparation of compounds **1**−**8** has been previously reported.[10] The ^{1}H and ^{13}C NMR spectra were recorded on a Varian Associates Gemini-200, Inova-300, or General Electric QE-300 spectrometer and referenced to protio impurities of commercial benzene-d_6 (C_6D_6) or toluene-d_8 (C_7D_8) as internal standards. Elemental analyses and molecular structures were obtained through Purdue in-house facilities.

[CpTi(OC_6HPh_2-2,6-Me_2-3,5)Me_2] (9). A sample of **1** (1.5 g, 3.3 mmol) was dissolved in benzene. This solution was stirred as LiMe (216 mg, 9.8 mmol) was slowly added. The solution was stirred for approximately 2 h and filtered, and the filtrate was evacuated to dryness, affording a yellow solid. Recrystallization from benzene/pentane afforded a yellow powder (1.36 g, 76%). Anal. Calcd for $C_{27}H_{28}OTi$: C, 77.88; H, 6.78. Found: C, 77.57; H, 6.73. ^{1}H NMR (C_6D_6, 30 °C): δ 7.07−7.29 (aromatics); 6.82 (s, *p-H*); 5.63 (s, *Cp*); 2.09 (s, *m-Me*); 0.26 (s, Ti−*Me*). Selected ^{13}C NMR (C_6D_6, 30 °C): δ 161.1 (Ti−O−*C*); 113.7 (*Cp*); 56.1 (Ti−*Me*); 20.8 (*m-Me*).

[CpTi(OC_6HPh_2-2,6-Bu^t_2-3,5)Me_2] (10). To a stirred solution of **2** (0.41 g, 0.76 mmol) in toluene (25 mL) was added LiMe (0.035 g, 1.59 mmol). The solution was stirred for 24 h and filtered, and the solvent was removed under vacuum, giving **10** as a yellow solid (0.36 g, 95%). ^{1}H NMR (C_6D_6, 30 °C): δ 7.71 (s, *p-H*); 7.02−7.31 (aromatics); 5.75 (s, *Cp*); 1.29 (s, C*Me*$_3$); 0.10 (s, Ti−*Me*). Selected ^{13}C NMR (C_6D_6, 30 °C): δ 163.0 (Ti−O−*C*); 147.5, 140.8, 132.6, 130.9, 128.3, 126.9, 118.7 (aromatics); 113.5 (*Cp*); 56.9 (*Me*); 37.4, (*C*Me$_3$); 33.1 (C*Me*$_3$).

[CpTi(OC_6HNp_2-2,6-Bu^t_2-3,5)Me_2] (11). To a stirred solution of **3** (0.54 g, 0.84 mmol) in toluene (25 mL) was added LiMe (0.055 g, 2.51 mmol). The solution was stirred for 24 h and filtered, and the solvent was removed under vacuum, giving **11** as a yellow solid (0.35 g, 69%). ^{1}H NMR (C_6D_6, 30 °C): δ 7.90 (s, *p-H*); 7.15−7.62 (aromatics); 5.17 (s, *Cp*); 1.21 (s, C*Me*$_3$); −0.35, −0.81, (s, Ti−*Me*). Selected ^{13}C NMR (C_6D_6, 30 °C): δ 163.6 (Ti−O−*C*); 152.0, 148.7, 138.9, 135.1, 134.0, 129.7, 126.0, 125.3, 119.9 (aromatics); 113.3 (*Cp*); 56.5, 56.1 (Ti−*Me*); 37.7 (*C*Me$_3$); 32.0 (C*Me*$_3$).

[CpTi(OC_6H_2Ph-2-Bu^t_2-4,6)Me_2] (12). A sample of **4** (2.0 g, 4.3 mmol) was dissolved in benzene. This solution was stirred as LiMe was slowly added (284 mg, 12.9 mmol). The solution was stirred for approximately 2 h and filtered, and the filtrate was evacuated to dryness, affording a yellow solid. Recrystallization attempts from benzene/pentane afforded a yellow powder (1.04 g, 58%). Anal. Calcd for $C_{27}H_{36}OTi$: C, 76.40; H, 8.55. Found: C, 76.12; H, 8.67. ^{1}H NMR (C_6D_6, 30 °C): δ 6.70−7.60 (aromatics); 5.57 (s, *Cp*); 1.68 (s), 1.32 (s, C*Me*$_3$); 0.85 (s, Ti−*Me*). Selected ^{13}C NMR (C_6D_6, 30 °C): δ 160.8 (Ti−O−*C*); 114.4 (*Cp*); 58.4 (Ti−*Me*); 35.8, 34.5 (*C*Me$_3$); 31.7, 30.5 (C*Me*$_3$).

[CpTi(OC_6H_2Np-2-Bu^t_2-4,6)Me_2] (13). A sample of **5** (2.0 g, 3.9 mmol) was dissolved in benzene. This solution was stirred as LiMe was slowly added (0.27 g, 11.6 mmol). The solution was stirred for approximately 1 h and filtered, and the filtrate was evacuated to dryness, affording a yellow solid, which was recrystallized from pentane to give **13** as yellow

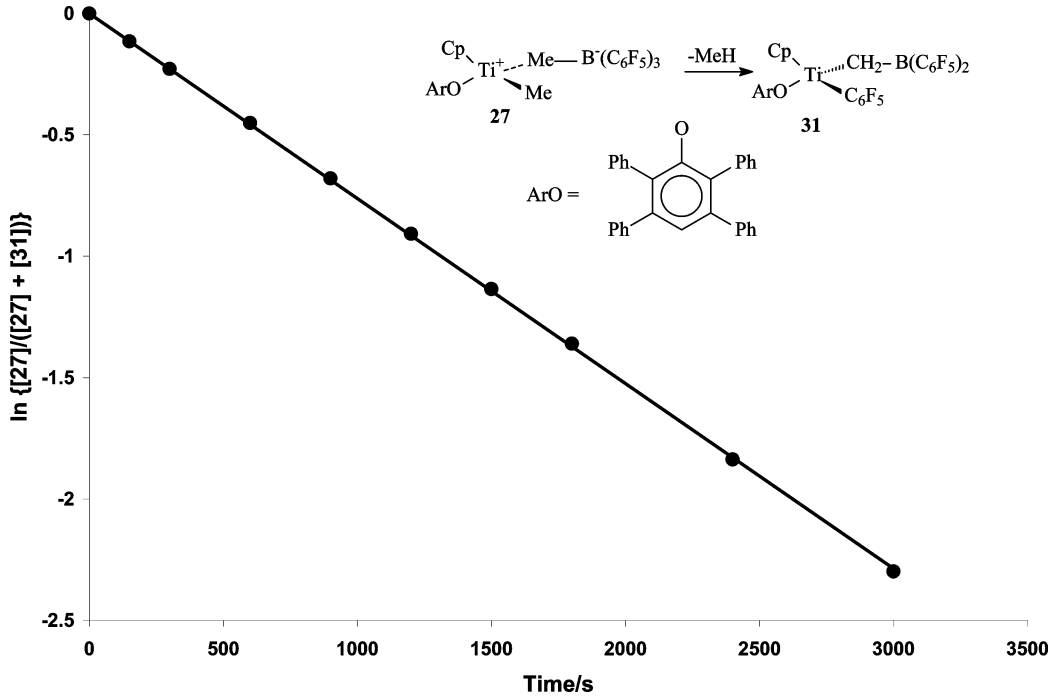

Figure 12. Plot of ln{[**27**]/([**27**] + [**31**])} vs time (in s) for the disappearance of **27** generated in situ from **17** and $[B(C_6F_5)_3]$. $[\mathbf{17}]_0 = 0.106$ M.

crystals (1.04 g, 58%). Anal. Calcd for $C_{31}H_{38}OTi$: C, 78.47; H, 8.07. Found: C, 78.59; H, 8.64. ^{1}H NMR (C_6D_6, 30 °C): δ 7.10−8.00 (aromatics); 5.41 (s, *Cp*); 1.64 (s), 1.26 (s, C*Me*$_3$); 0.58 (s), 0.15 (s, $^1J(^{13}C-^1H) = 124.0$, 123.1 Hz, Ti−*Me*). Selected ^{13}C NMR (C_6D_6, 30 °C): δ 161.6 (Ti−O−*C*); 114.1 (*Cp*); 58.4, 57.8 (Ti−*Me*); 35.8, 34.6 (*C*Me$_3$); 31.7, 30.6 (C*Me*$_3$).

[CpTi(OC$_6$H$_2${C$_{10}$H$_9$}-2-Bu$^t_2$-4,6)Me$_2$] (14). A sample of **6** (1.00 g, 1.93 mmol) was dissolved in benzene. This solution was stirred as LiMe was slowly added (0.128 g, 5.82 mmol). The solution was stirred for 24 h and filtered, and the filtrate was evacuated to dryness, affording a yellow glassy solid, which was recrystallized from pentane to give **14** as a yellow solid (0.92 g, 52%). Anal. Calcd for $C_{31}H_{40}OTi$: C, 78.13; H, 8.46. Found: C, 78.11; H, 8.66. ^{1}H NMR (C_6D_6, 30 °C): δ 7.56 (d), 7.22 (d, $^4J = 2.4$ Hz), 6.90−7.15 (aromatics); 5.92 (t, C*H*); 5.80 (s, *Cp*); 2.60 (m), 2.10 (m, CH_2CH_2); 1.58 (s), 1.26 (s, C*Me*$_3$); 0.80 (s), 0.54 (s, Ti−*Me*). Selected ^{13}C NMR (C_6D_6, 30 °C): δ 161.8 (Ti−O−*C*); 114.3 (*Cp*); 58.6, 57.0 (Ti−*Me*); 35.7, 34.5 (*C*Me$_3$); 31.7, 30.6 (C*Me*$_3$); 28.0, 23.6 (*C*H$_2$*C*H$_2$).

[Cp*Ti(OC$_6$HPh$_2$-2,6-Bu$^t_2$-3,5)Me$_2$] (15). To a stirred solution of **7** (0.23 g, 0.38 mmol) in benzene (10 mL) was added LiMe (0.035 g, 1.59 mmol). The solution was stirred for 24 h and filtered, and the solvent was removed under vacuum. The remaining orange powder was recrystallized as X-ray-quality crystals from a minimum amount of hexane, giving **15** (0.09 g, 41%). Anal. Calcd for $C_{38}H_{50}OTi$: C, 79.98; H, 8.83. Found: C, 80.18; H, 8.97. ^{1}H NMR (C_6D_6, 30 °C): δ 7.75 (s, *p-H*); 7.10−7.04 (aromatics); 1.58 (s, C$_5$*Me*$_5$); 1.26 (s, C*Me*$_3$); 0.03 (s, Ti−*Me*). Selected ^{13}C NMR (C_6D_6, 30 °C): δ 162.9 (Ti−O−*C*); 148.2, 141.3, 133.8, 131.9, 128.7, 127.3, 127.2, 122.5 (aromatics); 119.6 (*C*$_5$Me$_5$); 60.1 (Ti−*Me*); 38.0 (*C*Me$_3$); 33.8 (C*Me*$_3$); 12.3 (C$_5$*Me*$_5$).

[Cp*Ti(OC$_6$HPh$_4$-2,3,5,6)Me$_2$] (16). A solvent-sealed flask was charged with **8** (300 mg, 0.46 mmol), solid LiMe (30 mg, 1.4 mmol), and benzene. This mixture was stirred until the red solution turned dark yellow (at least 24 h) and filtered, and the solvent was removed under vacuum, affording a yellow solid, which could be recrystallized from benzene/pentane to give yellow crystals (80 mg, 28%). Anal. Calcd for $C_{42}H_{42}OTi$: C, 82.61; H, 6.93. Found: C, 82.40; H, 6.93. ^{1}H NMR (C_6D_6, 30 °C): δ 6.84−7.42 (aromatics); 1.40 (s, C$_5$*Me*$_5$); 0.27 (s, Ti−*Me*). Selected ^{13}C NMR (C_6D_6, 30 °C): δ 159.9 (Ti−O−*C*); 122.2 (*C*$_5$Me$_5$); 59.5 (Ti−*Me*); 11.1 (C$_5$*Me*$_5$).

[CpTi(OC$_6$HPh$_4$-2,3,5,6)Me$_2$] (17). A diethyl ether solution of $CpTiCl_3$ (0.50 g, 2.3 mmol) was cooled to −78 °C in a dry ice/acetone bath. To this solution was added LiMe (4.7 mL, 1.6 M in diethyl ether) via syringe under a flush of nitrogen. After the mixture was stirred for approximately 4 h, 2,3,5,6-tetraphenylphenol (0.91 g, 2.3 mmol) was added with stirring. The mixture was slowly warmed to room temperature and was stirred overnight. The solvent was removed under vacuum, and benzene was added to the solid residue. The suspension was filtered through a plug of Celite over fritted glass to remove the lithium salts. The filtrate was then evacuated to dryness, yielding a pale yellow powder (0.91 g, 75%). Anal. Calcd for $C_{37}H_{32}OTi$: C, 82.22; H, 5.97. Found: C, 82.06; H, 5.91. ^{1}H NMR (C_6D_6, 25 °C): δ 6.87−7.34 (aromatics); 5.53 (s, *Cp*); 0.33 (s, Ti−*Me*). Selected ^{13}C NMR (C_6D_6, 25 °C): δ 161.3 (Ti−O−*C*); 113.8 (*Cp*); 57.5 (Ti−*Me*).

[CpTi(OC$_6$Ph$_4$-2,3,5,6-Br-4)Me$_2$] (18). A diethyl ether solution of $CpTiCl_3$ (1.03 g, 4.70 mmol) was cooled to −78 °C in a dry ice/acetone bath. To this solution was added LiMe (9.1 mL, 1.6 M in diethyl ether) via syringe under a flush of nitrogen. After the mixture was stirred for approximately 4 h, 4-bromo-2,3,5,6-tetraphenylphenol (2.47 g, 5.17 mmol) was added with stirring. The mixture was slowly warmed to room temperature and was stirred overnight. The solvent was removed under vacuum, and benzene was added to the solid residue. The suspension was filtered through a plug of Celite over fritted glass to remove the lithium salts. The filtrate was then evacuated to dryness, yielding a pale yellow powder (2.14 g, 74%). Slow cooling of a saturated benzene solution afforded X-ray-quality crystals of the title compound as a benzene solvate. Anal. Calcd for $C_{37}H_{31}BrOTi$: C, 71.74; H, 5.04; Br, 12.90. Anal. Calcd for $C_{37}H_{31}BrOTi{\cdot}C_6H_6$: C, 74.04; H, 5.35; Br, 11.45. Found: C, 72.23; H, 5.33; Br, 12.37. ^{1}H NMR (C_6D_6, 25 °C): δ 6.72−7.29 (aromatics); 5.61 (s, *Cp*); 0.31 (s, Ti−*Me*). Selected ^{13}C NMR (C_6D_6, 25 °C): δ 160.3 (Ti−O−*C*); 114.0 (*Cp*); 57.9 (Ti−*Me*).

[CpTi(OC$_6$H$_3$Me$_2$-2,6)Me$_2$] (19). LiMe (9.0 mL, 1.6 M sol. in diethyl ether, 14.4 mmol) was added dropwise to a precooled suspension of $CpTiCl_3$ (1.00 g, 4.56 mmol) in 30 mL of Et_2O at −78°C. After the mixture was stirred for approximately 4 h, a solution of 2,6-dimethylphenol (0.557 g, 4.60 mmol) in 10 mL of Et_2O was added dropwise at −78°C. The mixture was

slowly warmed to room temperature and was stirred overnight. The solvent was removed under vacuum, and benzene was added to the solid residue. The suspension was filtered through a plug of Celite over fritted glass to remove the lithium salts. The filtrate was then evacuated to yield a dark yellow liquid (0.91 g, 76%). The liquid is stored at −30 °C to prevent decomposition. ^{1}H NMR (C_6D_6, 25 °C): δ 6.98 (d, J = 7.2 Hz, 2H, *m*-H); 6.82 (t, J = 7.2 Hz, 1H, *p*-H); 5.82 (s, 5H, *Cp*); 2.17 (s, 6H, *o*-Me); 0.91 (s, 6H, Ti−*Me*). Selected ^{13}C NMR (C_6D_6, 25 °C): δ 163.8 (Ti−O−*C*); 114.0 (*Cp*); 54.0 (Ti−*Me*).

[CpTi(OC$_6$H$_2$Me$_2$-2,6-Br-4)Me$_2$] (20). LiMe (9.0 mL, 1.6 M sol. in diethyl ether, 14.4 mmol) was added dropwise to a precooled suspension of $CpTiCl_3$ (1.00 g, 4.56 mmol) in 30 mL of Et_2O at −78 °C. After the mixture was stirred for approximately 4 h, a solution of 4-bromo-2,6-dimethylphenol (0.916 g, 4.56 mmol) in 10 mL of Et_2O was added dropwise at −78 °C. The mixture was slowly warmed to room temperature and was stirred overnight. The solvent was removed under vacuum, and benzene was added to the solid residue. The suspension was filtered through a plug of Celite over fritted glass to remove the lithium salts. The filtrate was then evacuated to dryness, yielding a dark yellow liquid. Upon standing at room temperature for a few hours, the liquid solidified, giving a dark yellow solid (0.91 g, 76%). X-ray-quality crystals were picked out from this solid. The solid was stored at −30 °C to prevent decomposition. Anal. Calcd for $C_{15}H_{19}BrOTi$: C, 52.53; H, 5.54; Br, 23.29. Found: C, 52.25; H, 5.41; Br, 22.90. ^{1}H NMR (C_6D_6, 25 °C): δ 7.09 (s, 2H, *m*-H); 5.77 (s, 5H, *Cp*); 1.39 (s, 6H, *o*-Me); 0.87 (s, 6H, Ti−*Me*). Selected ^{13}C NMR (C_6D_6, 25 °C): δ 162.5 (Ti−O−*C*); 114.1 (*Cp*); 54.9 (Ti−*Me*).

[CpTi(OC$_6$H$_3$Pr$^i_2$-2,6)Me$_2$] (21). LiMe (9.0 mL, 1.6 M sol. in diethyl ether, 14.4 mmol) was added dropwise to a precooled suspension of $CpTiCl_3$ (1.00 g, 4.56 mmol) in 30 mL of Et_2O at −78 °C. After the mixture was stirred for 4 h, a solution of 2,6-diisopropylphenol (0.845 mL, 4.56 mmol) in 10 mL of Et_2O was added dropwise at −78 °C. The mixture was slowly warmed to room temperature and was stirred overnight. The solvent was removed under vacuum, and benzene was added to the solid residue. The suspension was filtered through a plug of Celite over fritted glass to remove the lithium salts. The filtrate was then evacuated to dryness, yielding a dark yellow liquid. The liquid was then frozen with liquid nitrogen for 1 min. Upon standing at room temperature, the liquid solidified, giving a clear yellow crystal (1.12 g, 77%). X-ray-quality crystals were picked out from this solid. Anal. Calcd for $C_{19}H_{28}OTi$: C, 71.30; H, 8.75. Found: C, 70.59; H, 8.83. ^{1}H NMR (C_6D_6, 25 °C): δ 7.11 (d, 2H, *m*-H); 7.01 (t, 1H, *p*-H); 5.92 (s, 5H, *Cp*); 3.35 (sept, 2H, C*H*Me$_2$); 1.23 (d, 12H, CH*Me*$_2$); 0.94 (s, 6H, Ti−*Me*). Selected ^{13}C NMR (C_6D_6, 25 °C): δ 161.3 (Ti−O−*C*); 114.0 (*Cp*); 54.2 (Ti−*Me*).

[CpTi(OC$_6$H$_3$Me$_2$-2,6)$_2$Me] (22). LiMe (9.0 mL, 1.6 M solution in diethyl ether, 14.4 mmol) was added dropwise to a precooled suspension of $CpTiCl_3$ (1.00 g, 4.56 mmol) in 30 mL of Et_2O at −78 °C. After the mixture was stirred for approximately 4 h, a solution of 2,6-dimethylphenol (1.11 g, 9.09 mmol) in 15 mL of Et_2O was added dropwise at −78 °C. The mixture was slowly warmed to room temperature and was stirred overnight. The solvent was removed under vacuum, and benzene was added to the solid residue. The suspension was filtered through a plug of Celite over fritted glass to remove the lithium salts. The filtrate was then evacuated to yield a yellow solid (1.45 g, 86%). Anal. Calcd for $C_{22}H_{26}O_2Ti$: C, 71.39; H, 7.02. Found: C, 71.50; H, 6.92. ^{1}H NMR (C_6D_6, 25 °C): δ 6.97 (d, J = 7.2 Hz, 4H, *m*-H); 6.81 (t, J = 7.2 Hz, 2H, *p*-H); 5.85 (s, 5H, *Cp*); 2.21 (s, 12H, *o*-Me); 1.34 (s, 3H, Ti−*Me*). Selected ^{13}C NMR (C_6D_6, 25 °C): δ 164.4 (Ti−O−*C*); 114.8 (*Cp*); 48.5 (Ti−*Me*).

[CpTi(OC$_6$H$_2$Me$_2$-2,6-Br-4)$_2$Me] (23). LiMe (9.0 mL, 1.6 M solution in diethyl ether, 14.4 mmol) was added dropwise to a precooled suspension of $CpTiCl_3$ (1.00 g, 4.56 mmol) in 30 mL of Et_2O at −78 °C. After the mixture was stirred for approximately 4 h, a solution of 4-bromo-2,6-dimethylphenol (1.83 g, 9.12 mmol) in 15 mL of Et_2O was added dropwise at −78 °C. The mixture was slowly warmed to room temperature and was stirred overnight. The solvent was removed under vacuum, and benzene was added to the solid residue. The suspension was filtered through a plug of Celite over fritted glass to remove the lithium salts. The filtrate was then evacuated to dryness, yielding a yellow liquid. Upon standing at room temperature for a few hours, the liquid solidified, giving a yellow solid (1.90 g, 79%). X-ray-quality crystals were picked out from this solid. Anal. Calcd for $C_{22}H_{24}Br_2O_2Ti$: C, 50.05; H, 4.55; Br, 30.26. Found: C, 50.16; H, 4.56; Br, 30.19. ^{1}H NMR (C_6D_6, 25 °C): δ 7.08 (s, 4H, *m*-H); 5.73 (s, 5H, *Cp*); 1.94 (s, 12H, *o*-Me); 1.23 (s, 3H, Ti−*Me*). Selected ^{13}C NMR (C_6D_6, 25 °C): δ 163.1 (Ti−O−*C*); 115.1 (*Cp*); 49.9 (Ti−*Me*).

[CpTi(OC$_6$HPh$_2$-2,6-Me$_2$-3,5)Me][MeB(C$_6$F$_5$)$_3$] (24). An NMR tube was charged with 30 mg (0.072 mmol) of **9**, 70 mg (0.14 mmol) of $B(C_6F_5)_3$, and 0.5 mL of C_6D_6 or C_7D_8. The tube was quickly placed in an ice/acetone bath until just prior to ^{1}H and ^{13}C NMR analysis. ^{1}H NMR (C_6D_6, 30 °C): δ 6.80−7.32 (aromatics); 6.74 (s, *p-H*); 5.44 (s, *Cp*); 1.90 (s, *m-Me*); 0.68 (br, Ti−*Me*); 0.53 (br, B−*Me*). ^{1}H NMR (C_7D_8, −20 °C): δ 6.63−7.14 (aromatics); 5.39 (s, *Cp*); 1.87 (s, *m-Me*); 0.67 (s, Ti−*Me*); 0.46 (br, B−*Me*). Selected ^{13}C NMR (C_6D_6, 30 °C): δ 162.5 (Ti−O−*C*); 119.3 (*Cp*); 113.0 (br, B−*Me*); 77.8 (Ti−*Me*); 19.9 (*m-Me*).

[CpTi(OC$_6$H$_2$Ph-2-Bu$^t_2$-4,6)Me][MeB(C$_6$F$_5$)$_3$] (25). An NMR tube was charged with 30 mg (0.071 mmol) of **12**, 72 mg (0.14 mmol) of $B(C_6F_5)_3$, and 0.5 mL of C_6D_6 or C_7D_8. The tube was quickly placed in an ice/acetone bath until just prior to ^{1}H and ^{13}C NMR analysis. ^{1}H NMR (C_6D_6, 30 °C): δ 6.87−7.45 (aromatics); 5.44 (s, *Cp*); 1.43 (br, Ti−*Me*); 1.34 (s), 1.19 (s, C*Me*$_3$); 0.90 (br, B−*Me*). ^{1}H NMR (C_7D_8, −10 °C): δ 6.91−7.40 (aromatics); 5.37 (s, *Cp*); 1.52 (s, Ti−*Me*); 1.32 (s), 1.16 (s, C*Me*$_3$); 0.94 (br, B−*Me*). Selected ^{13}C NMR (C_6D_6, 30 °C): δ 163.0 (Ti−O−*C*); 120.4 (*Cp*); 113.0 (br, B−*Me*); 77.7 (br, Ti−*Me*); 35.1, 34.4 (*C*Me$_3$); 30.8, 29.7 (C*Me*$_3$). Selected ^{13}C NMR (C_7D_8, −10 °C): δ 163.2 (Ti−O−*C*); 120.7 (*Cp*); 112.9 (br, B−*Me*); 77.4 (s, Ti−*Me*); 35.4, 34.7 (*C*Me$_3$); 31.1, 30.0 (C*Me*$_3$).

[CpTi(OC$_6$H$_2$Np-2-Bu$^t_2$-4,6)Me][MeB(C$_6$F$_5$)$_3$] (26). An NMR tube was charged with 30 mg (0.063 mmol) of **13**, 65 mg (0.13 mmol) of $B(C_6F_5)_3$, and 0.5 mL of C_6D_6 or C_7D_8. The tube was quickly placed in an ice/acetone bath until just prior to ^{1}H and ^{13}C NMR analysis. ^{1}H NMR (C_6D_6, 30 °C): δ 7.05−7.68 (aromatics); 5.36 (s, *Cp*); 1.32 (s), 1.19 (s, C*Me*$_3$); 0.91 (br, Ti−*Me*); 0.81 (br, B−*Me*). ^{1}H NMR (C_7D_8, −10 °C): δ 6.97−7.68 (aromatics); 5.27 (s, *Cp*); 1.31 (s), 1.15 (s, C*Me*$_3$); 0.96 (br, Ti−*Me*); 0.77 (br, B−*Me*). ^{1}H NMR (C_7D_8, −30 °C): δ 6.96−7.67 (aromatics); 5.23 (s, *Cp* major); 5.14 (s, *Cp* minor); 1.31 (s), 1.21 (s, C*Me*$_3$); 0.95 (br, Ti−*Me* major); 0.76 (br, B−*Me* major); 0.54 (br, B−*Me* minor). Selected ^{13}C NMR (C_6D_6, 30 °C): δ 163.3 (Ti−O−*C*); 119.9 (*Cp*); 113.1 (br, B−*Me*); 79.4 (br, Ti−*Me*); 35.1, 34.4 (*C*Me$_3$); 30.9, 30.0 (C*Me*$_3$).

[CpTi(OC$_6$HPh$_4$-2,3,5,6)Me][MeB(C$_6$F$_5$)$_3$] (27). An NMR tube was charged with 30 mg (0.056 mmol) of **17**, 30 mg (0.059 mmol) of $B(C_6F_5)_3$, and 0.5 mL of C_6D_6 or C_7D_8. The tube was quickly placed in an ice/acetone bath until just prior to ^{1}H and ^{13}C NMR analysis. ^{1}H NMR (C_7D_8, 25 °C): δ 6.85−7.29 (aromatics); 5.34 (s, *Cp*); 0.68 (br, Ti−*Me*/B−*Me*). ^{1}H NMR (C_7D_8, −20 °C): δ 6.83−7.30 (aromatics); 5.22 (s, *Cp*); 0.69(br, Ti−*Me*); 0.62 (br, B−*Me*). Selected ^{13}C NMR (C_7D_8, −20 °C): δ 162.8 (Ti−O−*C*); 119.7 (*Cp*); 113.0 (br, B−*Me*); 79.2 (s, Ti−*Me*).

[CpTi(OC$_6$HPh$_2$-2,6-Me$_2$-3,5)(C$_6$F$_5$)(CH$_2$B{C$_6$F$_5$}$_2$)] (28). A sample of **9** (210 mg, 0.50 mmol) was dissolved in benzene along with 420 mg (0.82 mmol) of [$B(C_6F_5)_3$], causing the formation of a dark solution. The mixture was allowed to react overnight and evacuated to dryness, giving a dark solid. This solid was extracted with pentane, and the red extract was allowed to sit undisturbed overnight, affording red crystals

Table 9. Crystal Data and Data Collection Parameters

	13	14	15	18	20	21	23	28
formula	$C_{31}H_{38}OTi$	$C_{31}H_{40}OTi$	$C_{38}H_{50}OTi$	$C_{37}H_{31}BrOTi\cdot C_6H_6$	$C_{15}H_{19}BrOTi$	$C_{19}H_{28}OTi$	$C_{22}H_{24}Br_2O_2Ti$	$C_{44}H_{24}BF_{15}OTi$
formula wt	474.55	476.56	570.72	697.58	343.13	320.33	528.15	912.37
space group	$P2_1/c$ (No. 14)	$I4_1/a$ (No. 88)	$P2_1/c$ (No. 14)	$P2_1/c$ (No. 14)	$P\bar{1}$ (No. 2)	$P2_1/n$ (No. 14)	$Pnma$ (No. 62)	$P\bar{1}$ (No. 2)
a, Å	13.1917(8)	31.586(1)	12.0726(2)	10.6104(2)	7.646(1)	7.4673(8)	8.2285(3)	12.2084(5)
b, Å	11.7251(6)		21.8004(6)	20.5655(6)	9.6760(7)	16.085(1)	20.9915(9)	12.3668(2)
c, Å	18.788(1)	10.805(4)	26.0711(4)	16.5745(5)	11.125(1)	15.237(1)	12.7159(6)	13.7876(5)
α, deg	90	90	90	90	67.703(4)	90	90	71.440(2)
β, deg	107.115(2)	90	102.123(1)	106.168(2)	82.617(5)	93.036(6)	90	84.811(1)
γ, deg	90	90	90	90	88.058(7)	90	90	83.982(2)
V, Å^3	2777.4(5)	10780.3(1)	6708.6(4)	3473.7(2)	755.10(15)	1827.6(3)	2196.40(16)	1958.9(2)
Z	4	16	8	4	2	4	4	2
ρ_{calcd}, g cm^{-3}	1.135	1.174	1.130	1.334	1.509	1.164	1.597	1.547
temp, K	296	193	203	150	150	150	150	203
radiation (wavelength)				Mo Kα (0.710 73 Å)				
R	0.064	0.049	0.052	0.036	0.028	0.063	0.035	0.052
R_w	0.166	0.097	0.130	0.077	0.069	0.157	0.074	0.126

(140 mg, 30%). Anal. Calcd for $C_{44}H_{24}BF_{15}OTi$: C, 57.93; H, 2.65. Found: C, 57.77; H, 2.59. ^{1}H NMR (C_6D_6, 30 °C): δ 6.85−7.18 (aromatics); 6.68 (s, *p-H*); 5.65 (s, *Cp*); 3.56 (br), 2.67 (br, Ti−CH_2−B); 1.84 (s, *m-Me*). Selected ^{13}C NMR (C_6D_6, 30 °C): δ 162.3 (Ti−O−*C*); 118.1 (*Cp*); 114.2 (br, Ti−*C*H_2−B); 20.1 (*m-Me*).

[CpTi(OC$_6$H$_2$Ph-2-Bu$^t_2$-4,6)(C$_6$F$_5$)(CH$_2$B{C$_6$F$_5$}$_2$)] (29). A sample of **12** (200 mg, 0.47 mmol) was dissolved in benzene along with 362 mg (0.71 mmol) of B(C_6F_5)$_3$, causing the formation of a dark solution. The mixture was allowed to react overnight and evacuated to dryness, giving a dark solid. The solid was extracted with pentane, and the red extract was allowed to sit undisturbed overnight, affording red crystals (245 mg, 57%). Anal. Calcd for $C_{44}H_{32}BF_{15}OTi$: C, 57.42; H, 3.50. Found: C, 57.48; H, 3.26. ^{1}H NMR (C_6D_6, 30 °C): δ 7.56 (d), 7.13 (d, $^4J(^1H-^1H)$ = 2.5 Hz, *m-H*); 6.10 (s, *Cp*); 4.21 (br), 3.23 (br, Ti−CH_2−B); 1.62 (s), 1.26 (s, CMe_3). Selected ^{13}C NMR (C_6D_6, 30 °C): δ 163.7 (Ti−O−*C*); 119.4 (*Cp*); 107.1 (br, Ti−*C*H_2−B); 35.8, 34.7 (*C*Me$_3$); 31.4, 30.6 (C*Me*$_3$).

[CpTi(OC$_6$H$_2$Np-2-Bu$^t_2$-4,6)(C$_6$F$_5$)(CH$_2$B{C$_6$F$_5$}$_2$)] (30). A sample of **13** (200 mg, 0.42 mmol) was dissolved in benzene along with 324 mg (0.63 mmol) of B(C_6F_5)$_3$, causing the formation of a dark solution. The mixture was allowed to react for 4 h and then evacuated to dryness, giving a dark solid. The solid was extracted with pentane, and the red extract was allowed to sit undisturbed overnight, affording red crystals (160 mg, 39%). Anal. Calcd for $C_{48}H_{34}BF_{15}OTi$: C, 59.40; H, 3.53. Found: C, 59.28; H, 3.97. ^{1}H NMR (C_6D_6, 30 °C): δ 6.72−7.86 (aromatics); 6.24 (s), 5.80 (s, *Cp*); 4.16 (br), 4.14 (br), 3.00 (m, Ti−CH_2−B); 1.60 (s), 1.57 (s), 1.19 (s), 1.15 (s, CMe_3). Selected ^{13}C NMR (C_6D_6, 30 °C): δ 164.4, 164.3 (Ti−O−*C*); 119.2, 119.0 (*Cp*); 107.0, 105.5 (br, Ti−*C*H_2−B); 35.9, 35.8, 34.7, 34.7 (*C*Me$_3$); 31.4, 31.4, 30.7, 30.6 (C*Me*$_3$).

CpTi(OC$_6$HPh$_4$-2,3,5,6)(C$_6$F$_5$)(CH$_2$B{C$_6$F$_5$}$_2$)] (31). The compound **21** was allowed to sit at room temperature for 2 h, and NMR analysis was performed. The sample was then allowed to sit undisturbed overnight, affording large orange crystals. The crystals were washed several times with benzene and pentane and dried under vacuum. Anal. Calcd for $C_{54}H_{28}BF_{15}OTi$: C, 62.58; H, 2.72. Found: C, 64.25; H, 3.21. ^{1}H NMR (C_7D_8, 25 °C): δ 6.63−7.30 (aromatics); 5.64 (s, *Cp*); 3.62 (br), 2.75 (br, Ti−CH_2−B). Selected ^{13}C NMR (C_7D_8, 25 °C): δ 162.2 (Ti−O−*C*), 118.8 (*Cp*), 115.3 (br, Ti−*C*H_2−B).

X-ray Data Collection and Reduction. Crystal data and data collection parameters are contained in Table 9. A suitable crystal was mounted on a glass fiber in a random orientation under a cold stream of dry nitrogen. Preliminary examination and final data collection were performed with Mo Kα radiation (λ = 0.710 73 Å.) on a Nonius Kappa CCD. Lorentz and polarization corrections were applied to the data.[22] An empirical absorption correction using SCALEPACK was applied.[23] Intensities of equivalent reflections were averaged. The structure was solved using the structure solution program PATTY in DIRDIF92.[24] The remaining atoms were located in succeeding difference Fourier syntheses. Hydrogen atoms were included in the refinement but restrained to ride on the atom to which they are bonded. The structure was refined in full-matrix least-squares, where the function minimized was $\sum w(|F_o|^2 - |F_c|^2)^2$ and the weight w is defined as $w = 1/[\sigma^2(F_o^2) + (0.0585P)^2 + 1.4064P]$, where $P = (F_o^2 + 2F_c^2)/3$. Scattering factors were taken from ref 25. Refinement was performed on an AlphaServer 2100 using SHELX-97.[26] Crystallographic drawings were carried out using the programs ORTEP[27] and ORTEP-3 for Windows version 1.076.[28]

Acknowledgment. Support for this research was provided by the National Science Foundation (Grant No. CHE-0078405) and by the U.S. Department of Energy, Office of Basic Energy Sciences, through the Catalysis Science Grant No. DE-FG02-03ER15466.

Supporting Information Available: X-ray crystallographic data for **13**−**15**, **18**, **20**, **21**, **23**, and **28** as CIF files. This material is available free of charge via the Internet at http://pubs.acs.org.

OM0341404

(22) McArdle, P. C. *J. Appl. Crystallogr.* **1996**, *239*, 306.
(23) Otwinowski, Z.; Minor, W. *Methods Enzymol.* **1996**, 276.
(24) Beurskens, P. T.; Admirall, G.; Beurskens, G.; Bosman, W. P.; Garcia-Granda, S.; Gould, R. O.; Smits, J. M. M.; Smykalla, C. The DIRDIF92 Program System; Technical Report; Crystallography Laboratory, University of Nijmegen, Nijmegen, The Netherlands, 1992.
(25) *International Tables for Crystallography*; Kluwer Academic: Dordrecht, The Netherlands, 1992; Vol. C, Tables 4.2.6.8 and 6.1.1.4.
(26) Sheldrick, G. M. SHELXS97: A Program for Crystal Structure Refinement; University of Gottingen, Gottingen, Germany, 1997.
(27) Johnson, C. K. ORTEPII; Report ORNL-5138; Oak Ridge National Laboratory, Oak Ridge, TN, 1976.
(28) Farrugia, L. J. *J. Appl. Crystallogr.* **1997**, *30*, 565.